EUROPEAN ORGANIZATION FOR NUCLEAR RESEARCH

Status Report to the ISOLDE and Neutron Time-of-Flight Committee

Characterization of the low-lying 0^+ and 2^+ states of ^{68}Ni

September 26, 2019

C. Sotty[1,2], P. Van Duppen[1], M. Huyse[1], L.M. Fraile[3], A. Andreyev[4], G. Benzoni[5], R. Borcea[2], M. Carmona[3], C. Costache[2], H. De Witte[1], F. Flavigny[1], L. Gaffney[1], T. Grahn[6,7], P.T. Greenless[6,7], U. Koester[8], R. Lica[2], H. Mach[9], N. Mărginean[2], R. Mărginean[2], C. Mihai[2], F. Negoiţă[2], A. Negreţ[2], C. Niţă[2], B. Olaizola[3], J. Pakarinen[6,7], S. Pascu[2], V. Paziy[3], E. Rapisarda[5], L. Stan[2], M. Stanoiu[2], O. Tenglad[10], T. Thomas[11], A. Turturică[2], J.M. Udias[3], V. Vedia[3], W.B. Walters[12], N. Warr[11] and the ISOLDE-RILIS teams.

[1] *Instituut voor Kern- en Stralingsfysica, K.U. Leuven, Leuven, Belgium*
[2] *"Horia Hulubei" National Institute for Physics and Nuclear Engineering, 077125 Magurele, Romania*
[3] *Grupo de Física Nuclear, Universidad Complutense, 28040 Madrid, Spain*
[4] *Department of Physics, University of York, Heslington, UK*
[5] *Istituto Nazionale di Fisica Nucleare, Sezione di Milano, Via Celoria 16, 20133 Milano, Italy*
[6] *Department of Physics, University of Jyväskylä, Jyväskylä, Finland*
[7] *Helsinki Institute of Physics, Helsinki, Finland*
[8] *Institut Laue-Langevin, Grenoble, France*
[9] *BP1, NCBJ - National Center for Nuclear Research, Otwock, Poland*
[10] *Instituto de Estructura de la Materia, Madrid, Spain*
[11] *Institut fuer Kernphysik, Universitaet zu Koeln, Koeln, Germany*
[12] *Department of Chemistry, University of Maryland, Maryland, USA*

Spokesperson: C. Sotty [*Christophe.Sotty@nipne.ro*], L.M. Fraile [*luis.fraile@cern.ch*]
Contact person: C. Sotty [*Christophe.Sotty@nipne.ro*]

Abstract:
The identification of three pairs of 0^+ and 2^+ states in ^{68}Ni (Z=28 and N=40) provides an ideal test bench to validate shell-model calculations and effective interactions developed for the nickel region, but also hints to triple shape coexistence that may even include strongly deformed structures. The aim of this proposal was to collect detailed spectroscopic data of the low-spin states of ^{68}Ni in order to characterise these triple pairs of 0^+ and 2^+ states, by measuring the γ decay branching ratios of the 0^+ and 2^+ states and the E0 transition strengths as well as the E2 transition rate of the 0^+_3 using the new ISOLDE Decay Station.
The proposal was divided in two parts. The first one made use of a mixed array containing highly-efficient clover type HPGe detectors supplemented with $LaBr_3$(Ce) and plastic scintillators for β particle detection. The second part of the experiment devised an experimental setup that consisted in a similar HPGe array together with a high resolution electron detector to determine the half-life of 0^+_3 states and the E0($0^+ \rightarrow 0^+$) decay branches. This second run has not been allocated beam time until now, so it has not been performed.
In the first experiment the low-spin states in ^{68}Ni were populated following the β decay of the low-J isomeric state in ^{68}Co ($T_{1/2}$=1.6 s). Since the direct production of this isomer is hampered at ISOLDE, a pure source of ^{68}Co was obtained in the decay of ^{68}Mn laser-ionised by RILIS, which follows the ^{68}Mn ($T_{1/2}$=28(4) ms) - ^{68}Fe ($T_{1/2}$=132(39) ms) decay chain. As the ground state of ^{68}Fe is a 0^+ state, the spin selection rules in β decay guaranteed a pure source of ^{68}Co low-J isomer. We present here the results from this first experimental run to try and evaluate the lifetime of the ^{68}Ni 0^+_3 state through its direct decay on the 2^+_1 state. The presence of a strong Ga contamination prevented the extraction of the above mentioned lifetime, however, a tentative limit has been determined. Despite the isobaric contamination, the dataset allowed to establish for the ^{68}Fe decay daughter a richer level scheme and tentative lifetimes using the Fast Timing electronic technique.

Allocated shifts: [24] shifts (split into [2] runs), Shifts used: [12], Remaining shifts: [12]

1 Introduction

Around the closed shells, the nuclei are found to exhibit spherical shapes at low excitation energies [1]. Since the shell gaps are large, the lowest excited states are expected to be located at high excitation energies. However, at the expense of deforming the nucleus, the residual proton-neutron interactions can result in stable excited states across the shell gap. This factual coexistence of spherical and deformed shapes are notably observed in the heavy Pb isotopes [2]. In that respect, the region around ^{68}Ni is of particular interest, having a magic shell (Z=28) and a semi-magic shell (N=40, smaller shell gap), see proposal [3].

Many theoretical studies were performed in the ^{68}Ni region aiming at understanding the phenomena of rapid shape change and shape coexistence onto low-lying energy structures. The phenomenological JUN45 interaction [4] with the valence space limited to $f_{5/2}$, $p_{3/2}$, $p_{1/2}$ and $g_{9/2}$ neutron single-particle orbits with the constrains of excluding any proton excitation across $f_{7/2}$ proved to be able to reproduce, in good agreement, the energy position for the 0^+_2, 2^+_1 and 0^+_3 states in the present region. Along with the qualitative reproduction of level energies, larger scale shell model calculations including $fpg_{9/2}d_{5/2}$ neutron/proton orbits using the LNPS effective interaction [5] and the Monte Carlo Shell Model (MCSM) using the A3DA interaction [6], predict the phenomenon of shape coexistence in the ^{68}Ni [7] notably within the three first excited 0^+ states. The identification of these 0^+ states (and the associated 2^+ states) in ^{68}Ni provides an ideal test bench to validate shell-model calculations and effective interactions developed for the region.

The aim of this proposal was to collect detailed spectroscopic data of the low-spin states of ^{68}Ni in order to characterise these triple pairs of 0^+ and 2^+ states, by measuring the γ decay branching ratios of the 0^+ and 2^+ states and the E0 transition strengths as well as the E2 transition rate of the 0^+_3 using the new ISOLDE Decay Station. The aim was to populate ^{68}Ni following the β decay of the low-J isomeric state in ^{68}Co ($T_{1/2}$=1.6 s), by producing a pure source of ^{68}Co isomer in the decay of ^{68}Mn laser-ionised by RILIS, which follows the ^{68}Mn ($T_{1/2}$=28(4) ms) - ^{68}Fe ($T_{1/2}$=132(39) ms) decay chain. Since the ground state of ^{68}Fe is a 0^+ state, the spin selection rules in β decay guaranteed a pure source of ^{68}Co low-J isomer. Therefore the low-lying structures of ^{68}Fe, ^{68}Co and ^{68}Ni nuclei were studied in the β^- decay chain of ^{68}Mn. While β decaying along its chain, the proton/neutron ratio increases, which allows us to explores the shape coexistence phenomenon from daughter to grand-daughter nuclei, going from well deformed to spherical-like cases.

The experiment was divided up in two separate runs, one designed to address the decaying branches and level lifetimes via fast-timing and gamma spectroscopy, and a second one aimed at electron conversion measurements. Only the first one has actually taken place, while the second part has never had allocated beam time.

2 Details of the experiment

In order to produce the purest manganese beam, 1.4-GeV protons from the Proton Synchrotron Booster were impinged on a UC_x target. The fission products diffused from the hot target into the ion source. Manganese atoms were selectively ionised by the three Nd:YAG-pumped dye lasers provided by the Resonance Ionisation Laser Ion Source (RILIS) system [8]. Despite the efforts of the target/RILIS/IDS teams, four trials were needed before to extract and transport a significant amount of ^{68}Mn, which postponed the run with several years.

In the meantime, an experiment was performed at the National Cyclotron Laboratory (NSCL) to study low-lying 0^+ levels in ^{68,70}Ni populated via β decay of ^{68}Fe and ^{70}Co nuclei produced by fragmentation [7]. The measurement of the ^{68}Ni 0^+_3 state gave a new half-life value of 0.57(5) ns by using a coincidence on the 478-keV transition. In addition, the previously unobserved $2^+_1 \rightarrow 0^+_2$ branching ratio allowed to established many new electric dipole transition strengths as well as to place limits on electric monopole transition strengths.

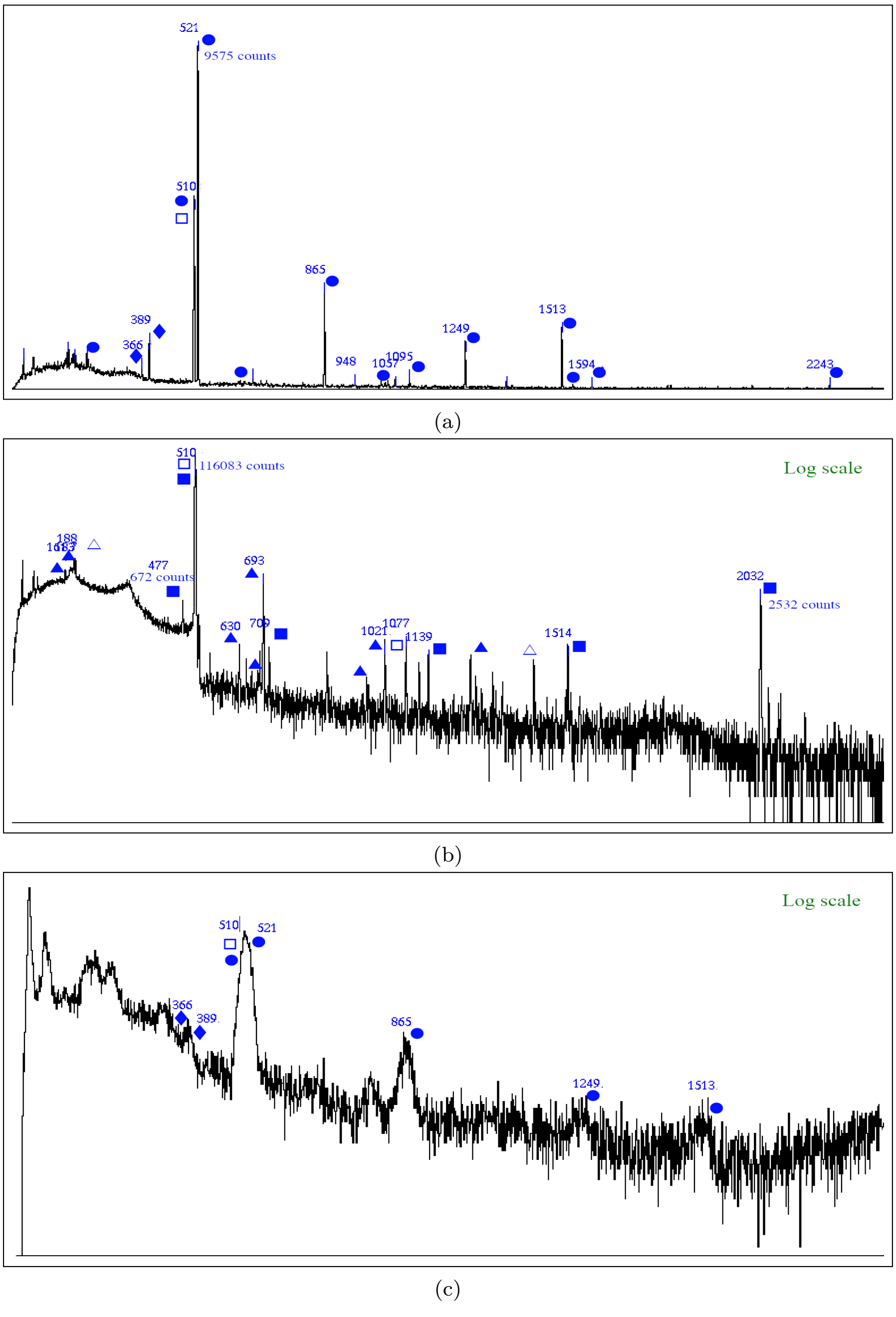

Figure 1: Typical β-gated γ-ray energy spectra of the ^{68}Mn β-decay chain for:
(a) the clovers array ; $T_P \in [1, 150]$ ms,
(b) the clovers array ; $T_P \in [200, 8000]$ ms,
(c) one LaBr$_3$ detector ; $T_P \in [1, 150]$ ms.
Symbols indicate lines associated with: (●) ^{68}Fe, (▲) ^{68}Co, (■) ^{68}Ni, (♦) ^{67}Fe, (△) ^{67}Co, (□) ^{68}Ga.

In the final attempt of the experment, since the production yields were too low using the neutron converter, the decision was taken to run directly on the primary target, at the expense of a large amount of isobaric $T_{1/2} = 67.71(8)$ min ^{68}Ga contamination. The cooler buncher ISCOOL was also problematic in the last attempts, so we chose the GPS for this last trial. The slits after the dipole magnets were used to reduce isobaric contaminants. Finally, the ions were implanted on an aluminized mylar tape located inside a movable tape station. The implantation point was immediately surrounded by one ΔE β detector and two $LaBr_3$(Ce) scintillators, and further four HPGe clover detectors. Signals were registered by the fully digital acquisition system, which was based on Nutaq cards coupled with a MIDAS framework [9].

In the energy spectra Fig. 1, it can be seen a strong presence of ^{68}Ga isobaric contribution which contaminates the 521-keV transition, $2_1^+ \rightarrow 0_1^+$ in ^{68}Fe(panels a and c). While the HPGe energy detectors present a good energy resolution and the 521-keV transition is observed as isolated; in the $LaBr_3$(Ce) scintillators, the transition together with the 511-keV are folded. The same case is encountered also for the 478-keV $0_3^+ \rightarrow 2{+}_1$ transition from ^{68}Ni. In Fig. 1 (panel b) for $T_P \in [200, 8000]$ ms, it can be observed that the 478-keV transition from ^{68}Ni is affected by a significant background given by the 511-keV annihilation. If the amount of statistics is consequent, this situation can be overcome by sorting β-gated γ spectra or β-gated $\gamma - \gamma$ matrices.

The tape cycle was based on the CERN proton Supercycle Structure (SC) to remove the long-lived activity. In our case, the SC contained up to 45 proton pulses, sent every 1.2s. In order to reduce the ^{68}Ga isobaric contamination, the beamgate was closed 150ms ($\sim$ 5$\times$ $T_{1/2}$(^{68}Mn)) after each proton pulses (PP). Subsequently, one shift was dedicated to the tuning of the target and line temperatures to improve the Mn/Ga ratio of around 30%. In addition, $laser-off$ data were acquired in order to identify the contributions from the contamination and potentially subtract them from laser-on spectra/matrices. The amount of statistics collected is around 30% lower than what we expected from the initial estimates, which already was at the edge of the technical feasibility. Due to different experimental conditions (mentioned above), the amount of Ga contamination highly perturbed the success of the measurement. A similar situation is expected for the proposed experiment addressing the electron conversion branch.

The clover HPGe and $LaBr_3$ detectors were calibrated in energy/time using standard spectroscopic and implanted sources respectively ^{152}Eu, ^{133}Ba, and, ^{138}Cs,^{88}Sr. Indeed, to correct the signal amplitude (energy) vs time dependence for the $LaBr_3$(Ce) scintillators induced by the CFDs in the electronics, standard sources can be employed. However, the offline standard spectroscopic source offers limited amount of prompt responses and sometimes with lifetime contribution coming from side feeding or high lying state. More prompt responses and a larger energy range can be obtained by implanting directly exotic ions in the tape using the target unit with proton beam.

3 Analysis and Results

3.1 Gamma spectroscopy and level schemes

The spectroscopic data obtained on the A=68 beta-decay allows to extend our knowledge on several nuclides. We concentrate here on results related to ^{68}Fe.
The decay scheme of ^{68}Fe following the β decay of ^{68}Mn (g.s.) has been built by using the γ-γ and β-gated γ-γ energy matrices with the coincidences techniques making full use of the HPGe detectors array. In order to minimize the background level related to the decay of daughter nuclei and taking into account the short half-life of ^{68}Mn, a gate applied on the time since proton impact (T_P) e.g. in between 1 ms and 150 ms (excluding the proton burst).Transitions associated with the decay of ^{68}Mn were also identified by comparing β-gated γ energy spectra with and without laser tuned to resonantly ionised Mn isotopes.

The intensities of the γ-ray transitions were determined based on β-γ coincidence spectrum and were normalized to the strongest transition at 521 keV. Relative intensities of γ-rays in ^{68}Co(g.s. direct feeding) and ^{67}Co(P_n) to the 521-keV line intensity have been determined to extract the total normalization factor. If one assumes that all excited levels decaying (directly or in cascades of γ-rays) are falling on the 521-keV state, which indicates that there is no high-energy γ-ray transition feeding directly the ground state, then the intensity of the 521-keV transition constitutes a good normalization reference. Since the

$Q_{\beta^-}(^{68}Mn) = 14530(920)$ keV value is large, the absolute values extracted for the β-direct feeding to ground state, probability of β^--delayed neutron emission and β feedings to the excited states should be considered as upper limits, and, their respective $\log(ft)$ values as lower limits due to the *pandemonium* effect [10]. The $\log(ft)$ values were determined using [11]. The ^{68}Mn ground state half-life was determined from the time-since-proton impact distribution gated on the most intense ^{68}Fe γ-rays, see Fig. 2.

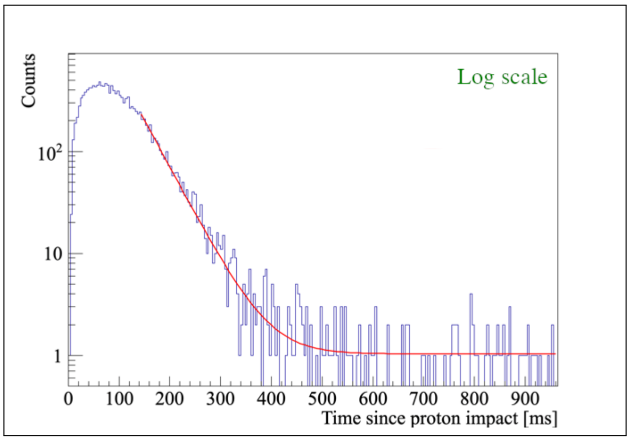

Figure 2: ^{68}Mn ground state half-life distribution. The time since proton impact curve is obtained by gating on the 521-, 864- and 866-, 1514-keV γ-rays originating from ^{68}Fe, detected using the HPGe clover array. The fit is performed outside the release time with beamgate closed.

Our analysis is consistent and greatly extending the previous level scheme for the ^{68}Fe nucleus [7,12–14], where only the 4 most intense γ-rays have been identified: 521 keV, 865 keV, 1249 keV and 1514 keV. From the systematics for the even-even Fe isotopic chain, see Fig. 3, correlating the experimental excitation energies with the determined branching ratios one can tentatively assign a spin $J^\pi = 4^-$ to the 1386-keV state in ^{68}Fe which is also supported by the assignment in Ref. [12]. Above the 4^+ state, it is less intuitive and rather difficult to point out the spins and parities without the support of theoretical calculations. As it can be noticed, across the even-mass Fe isotopic chain, the level of knowledge of spectroscopic observables above the first 4^+ state is quite low.

3.2 Lifetime analysis

The performance of time walk correction was needed since CFDs were used in the electronic chain and are well known to induce a time dependence with the energy of the γ-ray which needs to be software removed in the offline analysis [16]. Similarly, a time walk correction was made also for the β-LaBr$_3$(Ce) pairs of detectors. For this purpose, an online implanted ^{138}Cs source was used because it undergoes β^- decay ($I_\beta = 100\%$) to ^{138}Ba which decays through γ-ray radiation covering a range from 463 keV to 2640 keV [17]. For this study, the range is sufficiently large to perform the correction for $\gamma_{LaBr,STOP}$ energies from ^{68}Fe (521 keV, 864 and 866 keV, 1249 keV, 1514 keV) and from ^{68}Ni (478 keV). Similarly, the same correction was made for the LaBr$_3$(Ce)$_{START}$-LaBr$_3$(Ce)$_{STOP}$ combination, using an implanted ^{152}Eu source. Also in this case, the time walk correction spans over a wide energy interval, from about 244 keV to more than 1300 keV.

^{68}Ni

In order to determine the lifetime of the 2511-keV state, the couple $\gamma_{LaBr_3}(478)$-$\gamma_{LaBr_3}(1515)$ can be employed to obtain an estimation. But assuming negligible contribution in the centroid position coming from the β feeding or γ-rays populating the cascade, the amount of β-$\gamma_{LaBr_3}(478)$ coincidences can consist of a good probe to extract the partial half-life by gating on the 478-keV transition. The time deviation from the walk reference allows to determine a limit on the partial half-life. This estimation is

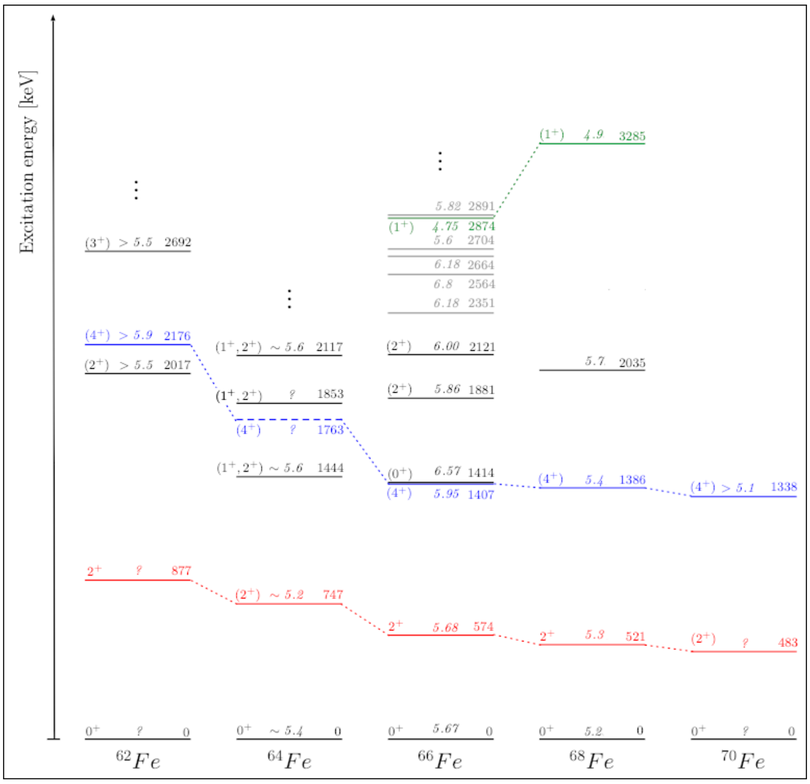

Figure 3: Systematics of the low-energy nuclear structure across even-mass $^{62-70}$Fe isotopic chain. The presented data is compiled from ENSDF [15].

consistent with the recently published value of 0.57(5) ns from Ref. [7].

^{68}Fe

Concerning the ^{68}Fe levels, one tried to extract the different half-live using the standard Fast Timing techniques Ref. [16]. The extraction of lifetimes was hampered by the 864-866 keV and 511-521 keV doublets. However, for the most intense 521-keV transition, one could apply an extra gate on the 1514-keV line in the HPGe. Limits could be established for the partial hall-lives of 521 keV and 1514 keV.

4 Summary

The A=68 isobaric chain has been produced starting from the decay of ^{68}Mn laser-ionised by RILIS, down to ^{68}Ni. In spite of the difficulties the lifetime of the 2511-keV state in ^{68}Ni has been estimated and is consistent with the latest value from [7].
Concerning the ^{68}Fe, the low-lying structure has been extended and lifetime limits have been established. A paper is in preparation on the results about ^{68}Fe, to be submitted to a peer reviewed journal. The discussion about its structure will be enlightened by MCSM and LNPS theoretical calculation as already performed in the ^{68}Ni region.
In the present conditions the measurement of conversion electrons as originally proposed will be very challenging, although new opportunities are offered by the SPEDE detector setup at the IDS.

References

[1] K. Heyde and J. L. Wood, Rev. Mod. Phys. **83**, 1467 (2011).

[2] A. N. Andreyev et al., Nature **405**, 430 (2000).

[3] C. Sotty and L. M. Fraile, INTC **Proposal** (2013).

[4] M. Honma, T. Otsuka, T. Mizusaki, and M. Hjorth-Jensen, Phys. Rev. C **80**, 064323 (2009).

[5] S. M. Lenzi, F. Nowacki, A. Poves, and K. Sieja, Phys. Rev. C **82**, 054301 (2010).

[6] Y. Tsunoda, T. Otsuka, N. Shimizu, M. Honma, and Y. Utsuno, Phys. Rev. C **89**, 031301 (2014).

[7] B. Crider et al., Physics Letters B **763** (2016).

[8] V. N. Fedosseev et al., Review of Scientific Instruments **83**, 02A903 (2012).

[9] MIDAS, Multi Instance Data Acquisition System , online.

[10] J. Hardy, L. Carraz, B. Jonson, and P. Hansen, Physics Letters B **71**, 307 (1977).

[11] NNDC, *Evaluated and Compiled Nuclear Structure Data Files*, online.

[12] G. Benzoni et al., Physics Letters B **751**, 107 (2015).

[13] P. Adrich et al., Phys. Rev. C **77**, 054306 (2008).

[14] S. N. Liddick et al., Phys. Rev. C **87**, 014325 (2013).

[15] NNDC, *EvaluatedNuclearStructureDataFile*, online.

[16] N. Mărginean et al., The European Physical Journal A **46**, 329 (2010).

[17] J. Chen, Nuclear Data Sheets **146**, 1 (2017).